Calculation of optical modes for chalcogenide compounds Sn2P2X6 (X=S, Se)

V.Yu. Klevets, N.D. Savchenko, A.G. Slivka, A.I. Susla, V.Yu. Bihanych
Uzhhorod National University, 88000, Uzhhorod, Voloshin Str., 54, Ukraine
e-mail: klevetsvyu@gmail.com

Fig. 1. The crystal structure of $Sn_2P_2S_6$ ferroelectric phase. The tin atoms positions in the paraelectric phase are shown by red. The shape of the Brillouin zone with denoted symmetrical points is shown for primitive monoclinic lattice[4]

Fig. 3. (a) Real and (b) imaginary parts of the dielectric function, reflecting the response of the (Bu, A′)-valence vibrations of $Sn_2P_2Se_6$ in its three phases[7]

Fig. 2. Fragment of the crystal structure of $Sn_2P_2Se_6$ ferroelectrics (a) and its corresponding Brillouin zone (b). The P-Se and P-P bonds inside the [P_2Se_6] group are shown. The atoms are, in decreasing size order, Se, P, and Sn. The numbers correspond to different independent crystallographic sites[8]

Bond lengths (nm) for the P_2Se_6 molecular unit in the ferroelectric phase (1), paraelectric phase (2) and data from [6] for paraelectric phase (3)

	1	2	3
P(l) -P(2)	0.2225(2)	0.2219(2)	0.222(1)
Se(l)-P(l)	0.2187(2)	0.2182(2)	0.2181(1)
Se(2)-P(l)	0.2192(2)	0.2187(3)	0.2191(1)
Se(3)-P(l)	0.2185(2)	0.2175(2)	0.2189(1)
Se(4)-P(2)	0.2182(2)		
Se(5)-P(2)	0.2198(2)		
Se(6)-P(2)	0.2184(2)		

Computational procedure and Results

Transverse optical and acoustic mode frequencies:

$$\omega_{TO,TA}^2 = \frac{\omega_0^2}{2}\left(1 \pm \sqrt{\cos^2\left(\frac{qa}{4}\right) + 0{,}44\sin^2\left(\frac{qa}{4}\right)}\right);$$

$$\omega_0^2 = \frac{64(1+\lambda)V_2\alpha_c^3}{3M_r d^2}; \quad \alpha_c = \frac{V_2}{\sqrt{V_2^2+V_3^2}}; \quad V_2 = \frac{\eta h^2}{m d^2},$$

where d – interatomic distance; α_c - covalency; M_r – energy equivalent of the reduced atomic mass., V_2 and V_3 – covalent and ionic bond energy, X=S, Se.

	Sn-X		P-X
	$V_3 = \frac{\varepsilon_{h+}-\varepsilon_{h-}}{2}$		$V_3 = \frac{\varepsilon_{p+}-\varepsilon_{p-}}{2}$
	$\eta_1 = \eta_{ss\sigma} + 2\sqrt{3}\eta_{sp\sigma} + 3\eta_{pp\sigma} = 3.22$		$\eta_2 = 2\sqrt{3}\eta_{sp\sigma} + 3\eta_{pp\sigma} = 2.89$
	$\lambda_1 = \frac{\sqrt{3}\eta_{sp\sigma}+3\eta_{pp\sigma}-3\eta_{pp\pi}}{-\eta_{ss\sigma}+2\sqrt{3}\eta_{sp\sigma}+3\eta_{pp\sigma}} = 0.854$		$\lambda_1 = \frac{3\eta_{pp\sigma}-3\eta_{pp\pi}}{-\eta_{ss\sigma}+2\sqrt{3}\eta_{sp\sigma}+3\eta_{pp\sigma}} = 0.663$

$$\eta_{sp\sigma} = 1.42, \quad \eta_{pp\sigma} = 2.22, \quad \eta_{ss\sigma} = -1.32, \quad \eta_{pp\pi} = -0.63$$

Table 1

Atomic terms and elemental atomic masses (M)

	Sn	P	S	Se
$-\varepsilon_p$, eV	6.76	9.54	11.60	10.68
$-\varepsilon_s$, eV	13.04	19.22	24.02	22.86
$-\varepsilon_h$, eV	8.33	9.54	14.71	13.73
M	118.7	30.97	32.06	78.96

Table 2

Experimental and calculated parameters for binaries

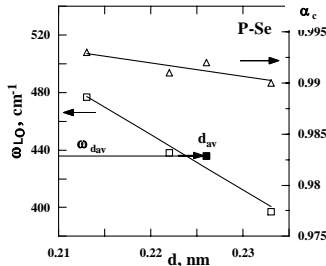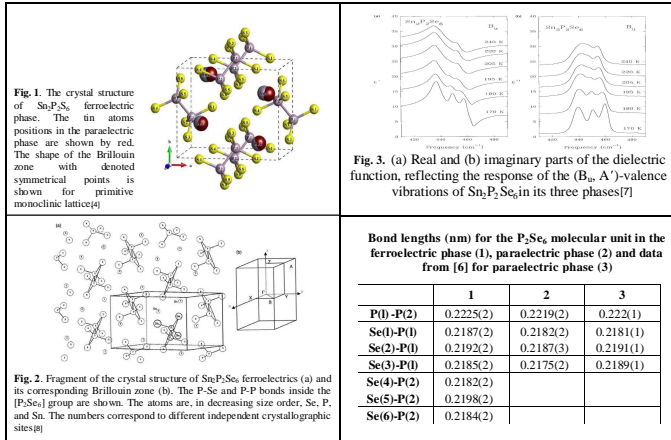| Parameters	Compound			
	PS	PSe	SnS	SnSe
d, nm	0.200	0.226	0.299	0.309
V_2, eV	5.51	4.44	3.44	2.59
V_3, eV	1.03	0.57	2.42	1.96
$(V_2^2+V_3^2)^{1/2}$, eV	5.43	4.48	4.21	3.25
α_c	0.92	0.99	0.82	0.80
M_r	15.72	22.24	25.24	47.42
ω_{LO}^{calc}, cm⁻¹	575	436	118	125
ω_{LO}^{exp}, cm⁻¹	555-591	454	137	134

Fig. 4. Calculated transverse optical mode frequencies and covalency versus interatomic distance for P-Se. Open squares show interatomic distances P-Se₁ (0.213 nm), P-Se₂ (0.224 nm), P-Se₃ (0.233 nm).
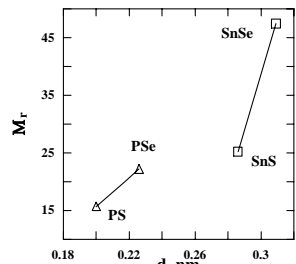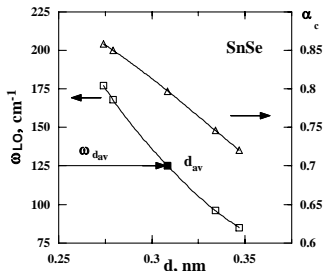

Fig. 5. Interatomic distance dependence of transverse optical mode frequencies and covalency for SnSe; d_1=(0.254 nm), d_2=(0.2567 nm), d_3=(0.334 nm), d_4=(0.347 nm)

Fig. 6. Correlation between covalency and interatomic distance for different chalcogenide compounds
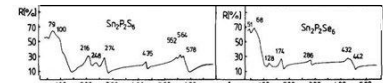
Fig. 7. FIR reflection spectra of layered hexachalcogenohypodiphosphates (pressed pellets, Bruker IFS 114) [3]

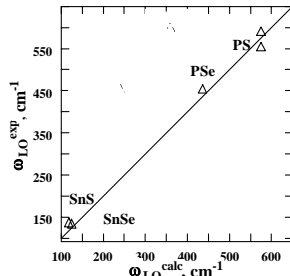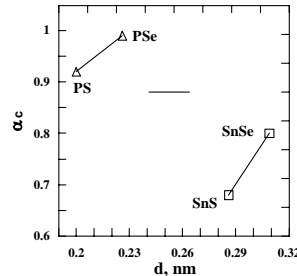Fig. 8. Correlation between the reduced mass and interatomic distance for different chalcogenide compounds

Fig. 9. Correlation between calculated and experimental values of longitudinal optical mode frequencies for chalcogenide compounds

References

[1] Harrison W. A., Elementary Electronic Structure. New Jersey, London, Singapore, Shanghai, Hong Kong, Taipei, Chennai: World Scientific Publishing Co. 2004.
[2] Kliche G. J. Sol. State Chem., 1984, 51, pp.118-126.
[3] Zamaraite I., Svirskas S., et al. Dielectric, pyroelectric and ferroelectric properties of lead-doped Sn2P2S6 crystals. Phase Transitions, 2019, v. 92, p. 500 - 507.
[4] Glukhov K., Fedyo K., Banys J., Vysochanskii Y. Electronic Structure and Phase Transition in Ferroelectric Sn2P2S6 Crystal. Int. J. Mol. Sci. 2012.
[5] Milutinovic A., Popovic Z.V., Tomic N., Devic S. Materials Science Forum, 2004, 453-454 pp. 299-304.
[6] Voroshilov Yu.V., et al. Sov. Phys. Crystallogr., 33, 761 1988.
[7] Eijt S., Maior M.M. J. Phys. and Chem. of Solids, 60, 631, 1999.
[8] R.Caracas et al. Phys. Rev. B 66, 104106, 2002